

Semi-automated application for estimating subthalamic nucleus boundaries and optimal target selection for deep brain stimulation implantation surgery

*John A. Thompson, PhD,¹ Salam Oukal,⁵ Hagai Bergman, MD, PhD,^{2,3} Steven Ojemann, MD,¹ Adam O. Hebb, MD,⁴ Sara Hanrahan, PhD,⁴ Zvi Israel, MD,³ and Aviva Abosch, MD, PhD¹

¹Department of Neurosurgery, University of Colorado School of Medicine, Aurora, Colorado; ²Department of Medical Neurobiology, The Hebrew University–Hadassah Medical School; ³Department of Neurosurgery, Hadassah Medical Center, Jerusalem, Israel; ⁴Colorado Neurological Institute, Englewood, Colorado; and ⁵Alpha Omega, Nazareth, Israel

OBJECTIVE Deep brain stimulation (DBS) of the subthalamic nucleus (STN) has become standard care for the surgical treatment of Parkinson's disease (PD). Reliable interpretation of microelectrode recording (MER) data, used to guide DBS implantation surgery, requires expert electrophysiological evaluation. Recent efforts have endeavored to use electrophysiological signals for automatic detection of relevant brain structures and optimal implant target location.

The authors conducted an observational case-control study to evaluate a software package implemented on an electrophysiological recording system to provide online objective estimates for entry into and exit from the STN. In addition, they evaluated the accuracy of the software in selecting electrode track and depth for DBS implantation into STN, which relied on detecting changes in spectrum activity.

METHODS Data were retrospectively collected from 105 MER-guided STN-DBS surgeries (4 experienced neurosurgeons; 3 sites), in which estimates for entry into and exit from the STN, DBS track selection, and implant depth were compared post hoc between those determined by the software and those determined by the implanting neurosurgeon/neurophysiologist during surgery.

RESULTS This multicenter study revealed submillimetric agreement between surgeon/neurophysiologist and software for entry into and exit out of the STN as well as optimal DBS implant depth.

CONCLUSIONS The results of this study demonstrate that the software can reliably and accurately estimate entry into and exit from the STN and select the track corresponding to ultimate DBS implantation.

<https://thejns.org/doi/abs/10.3171/2017.12.JNS171964>

KEYWORDS deep brain stimulation; subthalamic nucleus; basal ganglia; microelectrode recording; functional neurosurgery

Deep brain stimulation (DBS) of the subthalamic nucleus (STN) through an implanted multipolar electrode is a common treatment for advanced Parkinson's disease (PD).^{3,14,16,21} Optimal targeting of STN-DBS improves function via reducing motor symptoms—tremor, bradykinesia, and rigidity—by at least 50%, allowing for a significant decrease in levodopa dosage and levodopa-induced side effects.^{14,16,31} However, suboptimal targeting within the STN can give rise to intolerable sensorimotor side effects, such as dysarthria, contractions and pares-

thesias,^{4,8,36} eye movement perturbations, and psychiatric symptoms,^{15,18,23} limiting the management of motor symptoms. The small size of the STN motor territory and the consequences of spreading current to immediately adjacent structures obligate precise targeting. Neurosurgeons therefore rely on a combination of imaging, electrophysiology, kinesthetic responses, and stimulation testing to accurately place the DBS lead into the sensorimotor domain of STN.^{2,4,8}

At many centers around the world that treat movement

ABBREVIATIONS DBS = deep brain stimulation; DLOR = dorsolateral oscillatory region; MER = microelectrode recording; NRMS = normalized root mean square; PD = Parkinson's disease; STN = subthalamic nucleus; VMNR = ventromedial non-oscillatory region.

SUBMITTED August 9, 2017. **ACCEPTED** December 4, 2017.

INCLUDE WHEN CITING Published online May 18, 2018; DOI: 10.3171/2017.12.JNS171964.

* J. A. Thompson and S. Oukal have contributed equally to this work.

disorders, the gold standard for optimally targeting the sensorimotor area of the STN currently relies on micro-electrode recording (MER) of single and multi-neuron activity traversing the planned surgical trajectories.^{2,4,30} These recordings facilitate high-resolution mapping of the dorsal and ventral borders of STN, identify oscillatory patterns concordant with sensorimotor somatotopic receptive fields, and differentiate contiguous structures along the trajectory.^{1,13,25,27} However, interpretation of these electrophysiological patterns often relies on an experienced neurophysiologist, with the inherent problem of subjective interpretation.^{2,4} Moreover, single- and multi-neuron recordings are highly susceptible to patient-specific neuropathological aberrancies, ambient sources of noise, and fluid in the track.²⁹

Innovations to surmount some of the issues related to the use of MER for STN-DBS involve auto-detection of STN borders and prediction of the optimal target location for therapeutic benefit.^{12,28,30,34} Most solutions under development combine MER information with oscillatory patterns in specific frequency bands of the local field potential recordings.^{6,17,26,29} Notably, targeting areas within the STN that exhibit increases in beta frequency (13–30 Hz) spectral power correlates with improved postoperative outcome.³⁴

In this report, we assess the accuracy of a semi-automated application designed to detect the dorsal and ventral borders of the STN, as well as to predict the optimal implant depth, in comparison with the observations of an experienced neurosurgeon/neurophysiologist. We performed this assessment using 105 surgeries collected from 4 different neurosurgeons. All 3 sites used a simultaneous multi-track microelectrode (2–3 electrodes) recording approach. In our analysis, the software exhibited a high degree of concordance with the experienced neurosurgeon/neurophysiologist in detecting the dorsal and ventral borders of the STN, in predicting the optimal track from among the multi-electrode array, and in estimating the optimal implant depth for contact 0 (most ventral) of the DBS electrode, in all cases, with submillimetric agreement. These findings support the use of the tested software as an ideal adjunct to the neurosurgeon's current armamentarium for STN-DBS implantation surgeries.

Methods

This investigation was approved by an internal review board at each site. All analyses were conducted on de-identified data collected during the standard-of-care procedures for routine STN-DBS implantation surgery in patients with idiopathic PD, using retrospective chart review. As a retrospective review of de-identified data, this study did not require direct patient consent.

Population Demographics

Microelectrode recordings (MERs) from 81 patients with PD (58 males) undergoing STN-DBS implantation were collected and analyzed for this study (see Table 1). The patients' mean age (\pm SD) was 64.58 ± 7 years. All surgical patients met accepted selection criteria for STN-DBS, including a persistent positive response to anti-PD

TABLE 1. Patient demographics and surgery information

Characteristic	Value
All sites	
Total no. of patients	81
No. of male patients	58
F	23
Mean patient age in yrs (SD)	65 (7)
No. of cases	105
No. of tracks	219
Site 1	
Total no. of patients	38
No. of male patients	25
Mean patient age in yrs (SD)	66 (8)
No. of cases	52
No. of tracks	97
Site 2	
Total no. of patients	26
No. of male patients	19
Mean patient age in yrs (SD)	65 (6)
No. of cases	27
No. of tracks	61
Site 3	
Total no. of patients	18
No. of male patients	15
Mean patient age in yrs (SD)	62 (7)
No. of cases	26
No. of tracks	61

medications (> 30% improvement on the motor subscale of the Unified Parkinson's Disease Rating Scale, in the on vs off state), the absence of dementia on neuropsychological testing, and medical clearance for surgery.⁷

Study Design

The aim of this study was to assess the accuracy of a software tool (HaGuide Tool) in identifying entry into the STN, exit from the STN, the optimal implant track for DBS, and the optimal implant depth. The HaGuide Tool is a real-time algorithm implemented on the Neuro Omega system (Alpha Omega Engineering), designed to visually map the STN boundaries. In addition, the HaGuide Tool algorithm provides depth information related to defining the sensorimotor region of the STN, putatively located in the dorsolateral region and characterized by high theta (tremor related, 3–7 Hz) and beta (13–30 Hz) oscillations.^{32,34} The primary algorithm uses the normalized root mean square (NRMS) of the multiunit MER signal in conjunction with power spectrum analysis of the theta and beta oscillations as the main parameters for evaluating the STN boundaries.^{19,35} The NRMS sensitivity to changes in signal density assists in distinguishing the entry into and exit from the STN, according to the increase and decrease of the NRMS, while the power spectral density feature identifies the increase in theta and beta oscillations of the motor domain in PD patients (Fig. 1).

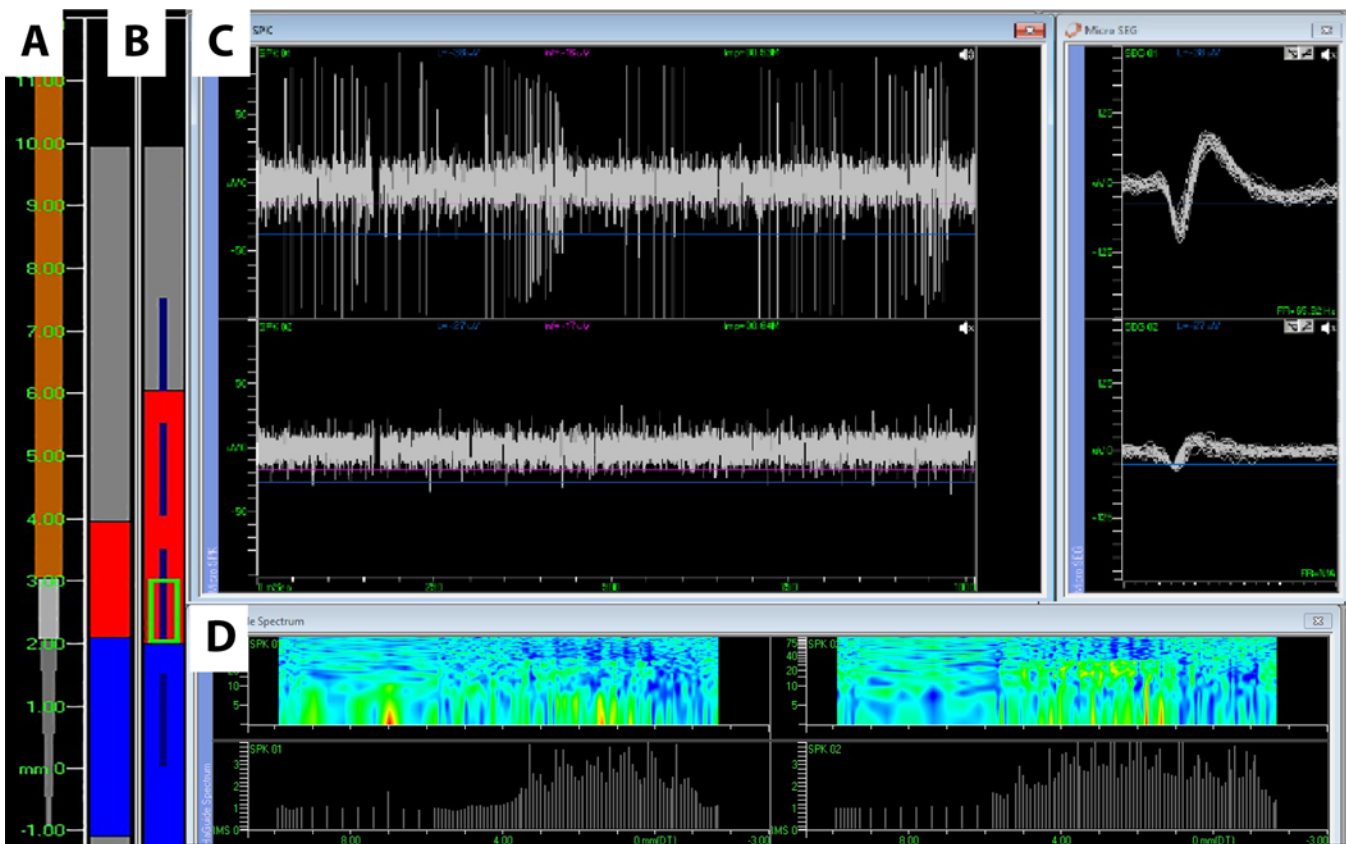


FIG. 1. **A:** Schematic of electrode tracks oriented from 11 mm above the target to the target—the ventral border of the STN. **B:** STN border classification indicated by color code: gray indicates non-STN; red indicates DLOR; blue indicates VMNR. **C:** Oscilloscope representation of voltage traces recorded from microelectrodes. **D:** The upper panels show color maps indicating the power spectrum from the recording locations, highlighting the beta-power spectrum. The bottom panels show bar plots of the root mean square calculated from the recording locations. Figure is available in color online only.

The data were collected from 3 study sites with relatively similar surgical strategies, although there were minor differences (detailed below). All surgeries followed the routine STN-DBS procedure employed for awake MER-guided implantation.² MER recordings in awake patients were performed using a single set of 2 or 3 parallel microelectrode tracks (separated by 2 mm using the cross-orientation in the 5-cannula microelectrode holder) per hemisphere. Neural data were acquired using the Neuro Omega intraoperative electrophysiological recording system. Trajectories from sites 2 and 3 started 25 mm above the putative target, which was defined as the ventral border of the STN as estimated by preoperative MRI, and used 3 simultaneous microelectrode tracks. Cases from site 1 were conducted using 2 simultaneous microelectrode tracks and started 10 mm above the target, as defined above.

In this study, an offline data-streaming tool was designed to automatically stream the surgery data to the HaGuide Tool on the Neuro Omega system, simulating a surgery. The raw recording data were converted and streamed to the Neuro Omega system, transferring digitized, filtered data for analysis by the HaGuide Tool algorithm. STN entry depth, STN exit depth, track selected for implantation, and implant depth were collected at the end of each simula-

tion. These results were compared post hoc to the operative chart notes collected by the expert DBS teams during the original surgery. All experts were blinded to the software output. For each STN entry, STN exit, STN total trajectory length, and implant depth, the absolute difference between the expert and HaGuide Tool results was calculated for each electrode trajectory. For optimal implant track selection, the percent agreement between the HaGuide Tool and the experts was calculated across all cases.

Data Acquisition

All collected and analyzed data were acquired from DBS surgeries using a Neuro Omega system. Raw and spiking signals were amplified by 20 \times , sampled at 44 kHz by a 16-bit A/D converter (using ± 1.25 V input range; i.e., $\sim 2\text{-}\mu\text{V}$ amplitude resolution). The raw signal was band-pass filtered from 0.7 to 9000 Hz, using a hardware 4-pole Butterworth filter. The spiking signal was band-pass filtered from 300 to 9000 Hz, using a hardware 4-pole Butterworth filter.

Statistical Analysis

Normality of all distributions was tested using an Anderson-Darling test of normality ($p < 0.05$). Statistical

tests used for paired comparisons or group comparisons were selected based on the outcome of the normality test. Non-normal paired comparisons were computed using a Mann-Whitney test, and normal distributions were compared with a paired t-test. For group comparisons, normal distributions were compared with a one-way ANOVA, and non-normal distributions were compared with a Kruskal-Wallis H-test. Group comparisons were followed by an appropriate post hoc test—Tukey's HSD for normally distributed group comparisons, and Dunn's test for non-parametric distribution comparisons. The strength of the relationship between surgeon/electrophysiologist and HaGuide for STN entry, exit, and total length, and implant depth was measured using Pearson's correlation.

Results

We replayed 105 previously collected surgery cases (219 electrode trajectories) through the Neuro Omega recording system, which allowed the software application to compute estimates for trajectory depth at entry into the STN, exit out of the STN, optimal implant track selection, and recommended optimal implant depth.

Detection of the Dorsal and Ventral Borders of the STN

As the initial test for the accuracy of the estimates generated by the application for individual electrode trajectories, we compared depth (relative to target) at which the entry into the STN and exit out of the STN were detected. Figure 2A compares the STN entry estimate distributions—in addition to the individual data points—from the experienced observer (blue) and the application (red). Comparing entry estimates with a nonparametric 2-sample test (Mann-Whitney) indicated that the medians were not significantly different ($U = 1.29$, $p = 0.2$; surgeon entry median = 4.79 mm, application entry median = 5.03 mm). Correlation analysis demonstrated a strong positive relationship between the surgeon and the application estimates for STN entry: $r(217) = 0.89$, $p = 4.74e-76$ (Fig. 2B). Figure 2C compares the STN exit estimate distributions—in addition to the individual data points—between the application and an experienced observer. Comparing exit estimates with a nonparametric 2-sample test (Mann-Whitney) indicated that the medians were not significantly different ($U = -1.59$, $p = 0.11$; surgeon exit median = -0.46 mm, application exit median = -0.76 mm). Correlation analysis demonstrated a strong positive relationship between the surgeon and the application estimates for STN exit: $r(217) = 0.89$, $p = 7.70e-75$ (Fig. 2D).

Figure 2E and F compares distributions derived from computing the absolute difference between surgeon estimates and the application, for entry into (gray) and exit from the STN (black); Fig. 2E represents unscaled data points, and Fig. 2F represents log-scaled data points. Comparison of the absolute difference estimates with a non-parametric two-sample test (Mann-Whitney) indicated that the medians were significantly different ($U = -2.26$, $p = 0.02$; entry difference median = 0.2 mm, exit difference median = 0.27 mm). Although the distributions were significantly different, the difference between median offsets was less than 0.1 mm.

In addition to comparing the estimates for entry into and exit from the STN, we compared the overall estimates of STN length between surgeon/electrophysiologist during each surgery and the application (Fig. 3A). Comparing STN length estimates with a nonparametric 2-sample test (Mann-Whitney) indicated that the medians were significantly different ($U = 2.80$, $p = 0.005$; surgeon STN length median = 5.3 mm, application STN length median = 5.7 mm). Although the distributions were significantly different, the difference between STN length median offsets was less than 0.5 mm. Overall greater variance in the estimate of STN exit may have contributed to the significant difference in STN length. In addition, correlation analysis demonstrated a strong positive relationship between the surgeon and the application estimates for STN length: $r(217) = 0.78$, $p = 7.35e-46$ (Fig. 3B).

Estimation of Optimal Implant Track and Optimal Implant Depth

All surgical cases re-examined in this study used a simultaneous multi-electrode strategy to implant the DBS lead. It is not uncommon with multi-track recordings for more than 1 track to traverse the STN, resulting in several options for DBS lead implantation. For this study, we first compared the percentage of tracks for which the application agreed with the surgeon—representing the ground truth—in selecting the optimal DBS implant track, and we found agreement in 84% of the tracks selected for implantation (184/219). Second, for these surgical cases in which the application agreed with the surgeon on implant track selection we compared the estimate for implant depth—meaning the depth at which to place the ventral tip of the ventral-most DBS contact (Fig. 4A). Comparing implant depth estimates with a parametric 2-sample test showed that the medians were significantly different ($t[85] = -3.51$, $p = 7.19e-4$; surgeon implant depth mean = -0.67 ± 1.12 mm, application implant depth mean = -0.96 ± 1.22 mm). Correlation analysis demonstrated a strong positive relationship between the surgeon and the application estimates for STN exit: $r(84) = 0.79$, $p = 1.21e-19$ (Fig. 4B). Analysis of the absolute difference for implant depth between surgical data and the application determination evidenced a mean of 0.63 mm (Fig. 4C).

The application interface displays information related to the estimation of the dorsolateral oscillatory region (DLOR) of the STN (red block in Fig. 1B) and the ventromedial non-oscillatory region (VMNR; blue block in Fig. 1B). Previous work has shown that increased beta (13–30 Hz) oscillatory activity in the STN is localized to a distinct boundary within the dorsolateral territory and correlates both with movement-related receptive fields and with the location of the therapeutic target for DBS stimulation.³⁴ We further sought to determine how well DLOR estimation derived from the application related to optimal therapeutic implant track selection (results summarized in Table 2). First, we examined whether tracks selected for implant versus those tracks not selected differed in the total length of DLOR. A paired t-test indicated that tracks selected for implant, on average, exhibited longer extents of DLOR ($t[170] = -2.64$, $p = 0.009$; implant track DLOR length = 3.10 ± 1.46 mm, non-implant track DLOR length

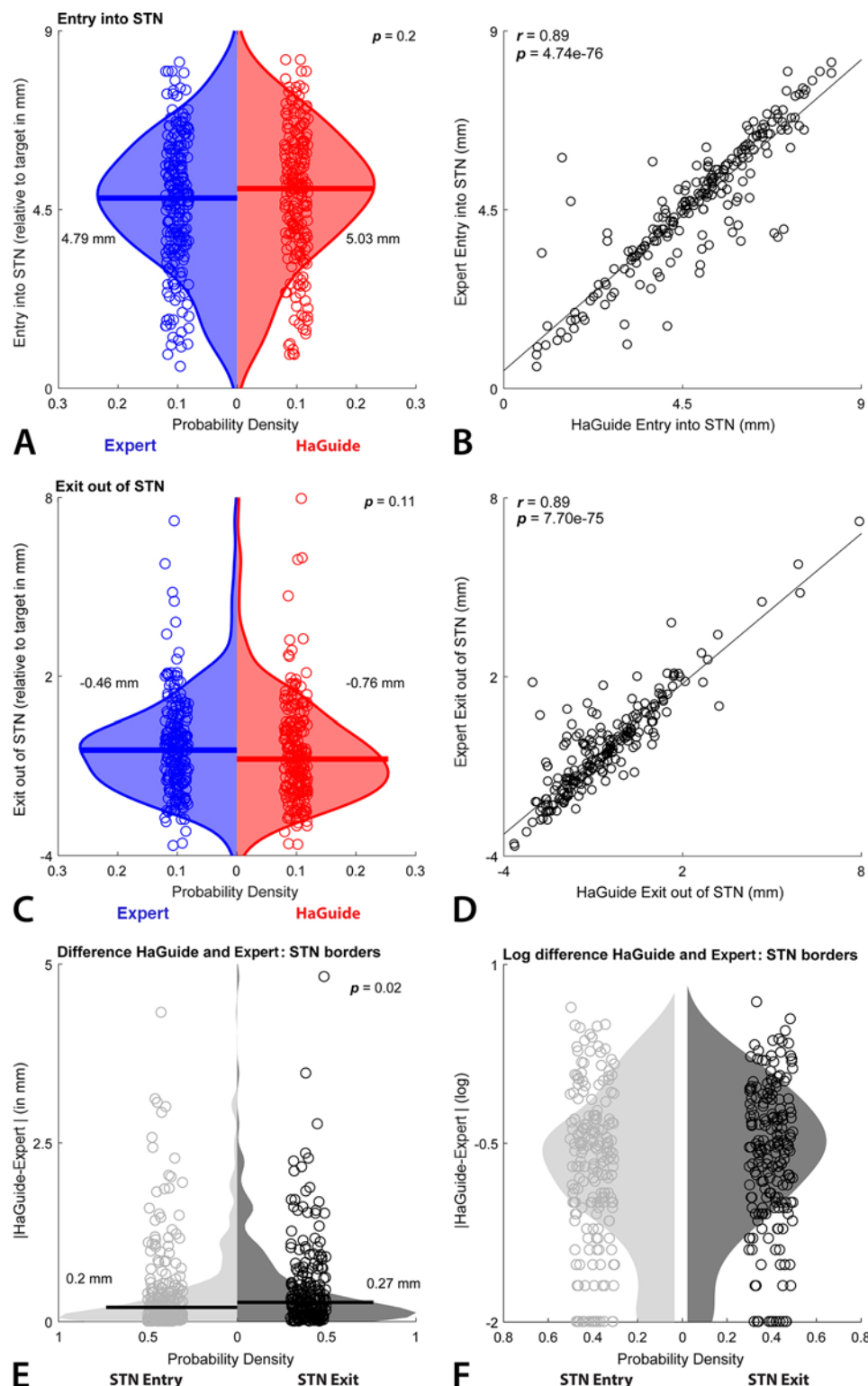


FIG. 2. **A:** Comparison of HaGuide and expert estimates for entry into the STN. The difference between the medians for the entry estimate distributions was 0.24 mm, and the distributions were not significantly different. **B:** Correlation between HaGuide and expert estimates for entry into the STN. HaGuide and expert estimates for entry were highly significantly correlated. **C:** Comparison of HaGuide and expert estimates for exit out of the STN. The difference between the medians for the exit estimate distributions was 0.3 mm, and the distributions were significantly different. **D:** Correlation between HaGuide and expert estimates for exit out of the STN. HaGuide and expert estimates for exit were highly significantly correlated. **E:** Comparison of the absolute differences for the entry into and exit from the STN. The difference between the medians for the entry estimate distributions was 0.24 mm, and the distributions were not significantly different. **F:** Comparison of the logarithmic absolute differences for the entry into and exit from the STN. Figure is available in color online only.

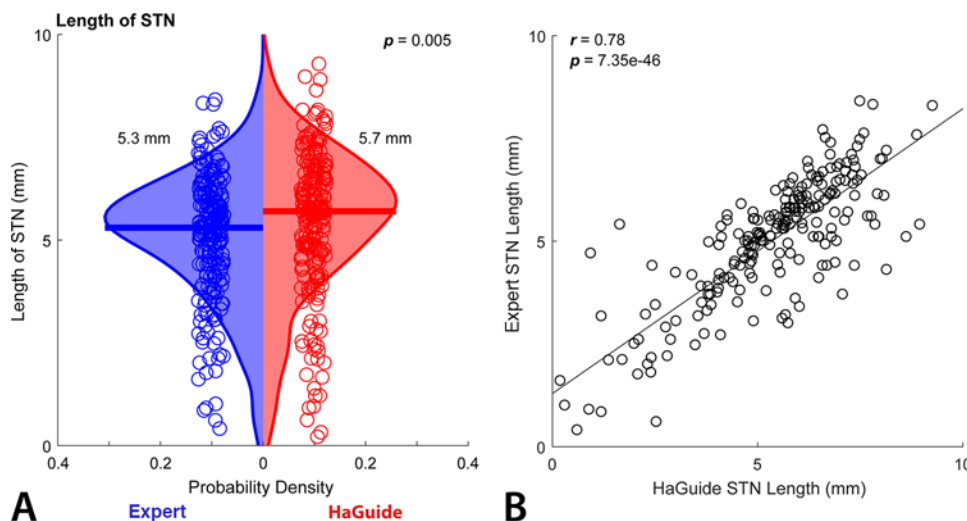


FIG. 3. **A:** Comparison of HaGuide and expert estimates for the length of the STN. The difference between the medians for the entry estimate distributions was 0.4 mm, and the distributions were significantly different. **B:** Correlation between HaGuide and expert estimates for the length of the STN. HaGuide and expert estimates for entry were highly significantly correlated. Figure is available in color online only.

$= 2.51 \pm 1.37$ mm). Second, we determined whether there was a predictive difference in the fraction of DLOR over the extent of STN. A paired t-test indicated that there was no difference in DLOR length as a fraction of total STN length between implant tracks and non-implant tracks ($t[170] = 0.76$, $p = 0.21$; implant track DLOR fraction $= 0.48 \pm 0.2$, non-implant track DLOR fraction $= 0.51 \pm 0.24$ mm). One of the more common parameters used to determine optimal impact in the context of multiple recordings is the total length of the STN. We further examined whether the application-indicated implant tracks differed

from non-implant tracks in total STN length. A paired t-test indicated that tracks selected for implant, on average, exhibited longer traversal through STN ($t[170] = -7.3$, $p = 5.3e-12$; implant track STN length $= 6.23 \pm 1.20$ mm, non-implant track STN length $= 4.70 \pm 1.80$ mm).

Study Site Differences

In a multisite study, differences in surgical approach and subjective interpretation of multiunit electrophysiological data, in addition to strategies to mitigate ambient noise present in the OR, will inevitably lead to unique dis-

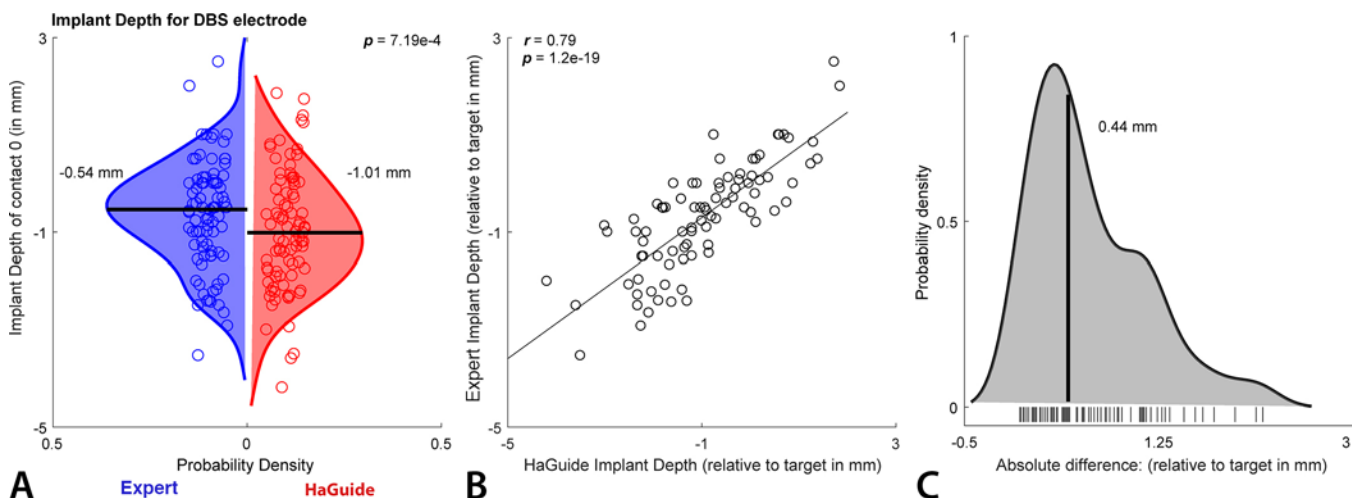


FIG. 4. **A:** Comparison of HaGuide and expert estimates for the implant depth of the DBS electrode. The difference between the medians for the entry estimate distributions was 0.47 mm, and the distributions were not significantly different. **B:** Correlation between HaGuide and expert estimates for the implant depth of the DBS electrode. HaGuide and expert estimates for the implant depth of the DBS electrode were highly significantly correlated. **C:** The absolute differences between HaGuide and expert estimates for the implant depth of the DBS electrode were on average less than 1 mm (median 0.44 mm). Hash marks below the probability density plot represent individual data points. Figure is available in color online only.

tributions of data for each site. We sought to determine the extent of the differences between study sites with regard to the absolute difference between the application and surgeon for STN entry, STN exit, and implant depth (Fig. 5A and B). We investigated the difference between sites for these parameters using a nonparametric one-way ANOVA (Kruskal-Wallis H-test). For STN entry, there were significant differences between site 3 and both site 2 and site 1, but not between site 1 and site 2 (site 3 vs site 1, $p = 0.004$; site 3 vs site 2, $p = 0.03$; site 1 vs site 2, $p = 0.2$; Fig. 5A). For STN exit, there were significant differences between site 3 and both site 2 and site 1, but not between site 1 and site 2 (site 3 vs site 1, $p = 0.005$; site 3 vs site 2, $p = 0.01$; site 1 vs site 2, $p = 0.8$; Fig. 5A). For implant depth, there were significant differences between site 2 and both site 1 and site 3, but not between site 1 and site 3 (site 2 vs site 1, $p = 0.001$; site 3 vs site 1, $p = 0.009$; site 1 vs site 3, $p = 0.9$; Fig. 5B).

Discussion

In this study, we have evaluated a novel software package that provides online objective estimation for STN entry and exit, as well as selection of the optimal implant track and depth selection for positioning the ventral-most contact of a DBS lead in the STN. The results were compared with real-time decisions of expert neurophysiologists and neurosurgeons. Our findings indicate that the software was reliable for detecting STN boundaries. On average, we found less than 0.24 mm mismatch for the STN entry and less than 0.3 mm mismatch for the STN exit. The total difference for depth implantation was less than 0.47 mm, and the total agreement on the optimal track was 84%.

Strategies to Identify STN Borders

Using MER, neurophysiologists employ visual and auditory features to delineate the dorsoventral boundary of the STN, which is identified by a sharp, distinctive increase in both background activity and spiking, multiunit neural activity. A similarly precipitous decline in activity marks the exit from the STN at the ventral border.^{13,19,20} Recently, several groups have used these STN features to develop computational machine learning approaches to auto-detect the boundaries of the STN.^{22,30,33,35} Reliable and consistent interpretation of MER findings requires a high level of expertise and is ultimately subject to human error. The software algorithm studied here, similar to previously published approaches for auto-detection of STN boundaries, depends mostly on the normalized root mean square (NRMS) value of the multiunit signal.³⁰ As indicated by the probability distributions for both the HaGuide and expert estimates of the STN borders in Fig. 2A and B, substantial variability is inherent to the detection of these anatomical locations. It is important to note that both the HaGuide software and human estimates account for the case-to-case variability and arrive at similar calculations (Fig. 2E and F)—one through algorithmic assessment of the electrophysiology and the other through an aggregated heuristic combining electrophysiology, somatosensory receptive fields, knowledge of neuroanatomy, and experience.

TABLE 2. Contributions to implant track selection

Parameter	Value
HaGuide implant track accuracy	
All tracks	84% (184/219)
Implant track	83% (87/105)
DLOR length & implant track	
DLOR length in mm	
Implant track, mean (SD)	3.10 (1.46)
Non-implant track, mean (SD)	2.51 (1.37)
Implant track vs non-implant track	
t statistic	-2.64
df	170
p value	0.009
DLOR fraction & implant track	
DLOR fraction	
Implant track, mean (SD)	0.48 (0.20)
Non-implant track, mean (SD)	0.51 (0.24)
Implant track vs non-implant track	
t statistic	0.76
df	170
p value	0.21
STN length & implant track	
STN length in mm	
Implant track, mean (SD)	6.23 (1.20)
Non-implant track, mean (SD)	4.70 (1.80)
Implant track vs non-implant track	
t statistic	-7.30
df	217
p value	5.30e-12

Boldface type indicates statistical significance.

Strategies to Identify Optimal Target Implant Depth

Despite heterogeneity among expert neurosurgeons and electrophysiologists in selecting the optimal DBS target localization within the STN for the treatment of PD, consensus tends to cluster around the dorsolateral region of the posterior STN.¹⁰ Standard intraoperative targeting of this region requires integration of several indirect measures, including stereotactic trajectory planning through indirect or direct identification of STN coordinates, detection of tremor-synchronous neural activity in STN, delineation of the dorsal-to-ventral extent of the STN, detection of active and passive movement-responsive neural activity in the STN, and responses to macrostimulation through the implanted DBS electrode.^{2,4} Recent efforts to generate automatic detection of optimal DBS electrode placement in the STN have used the enhanced beta-band power within the STN, an electrophysiological biomarker of PD, measured via local field potential recordings.^{5,11} Several groups have demonstrated that the increased beta-band power reliably identifies the dorsolateral STN and predicts motor symptom improvement in response to DBS.^{12,28,34} The software described here similarly uses changes in beta-band power to define motor and non-motor regions of the STN.

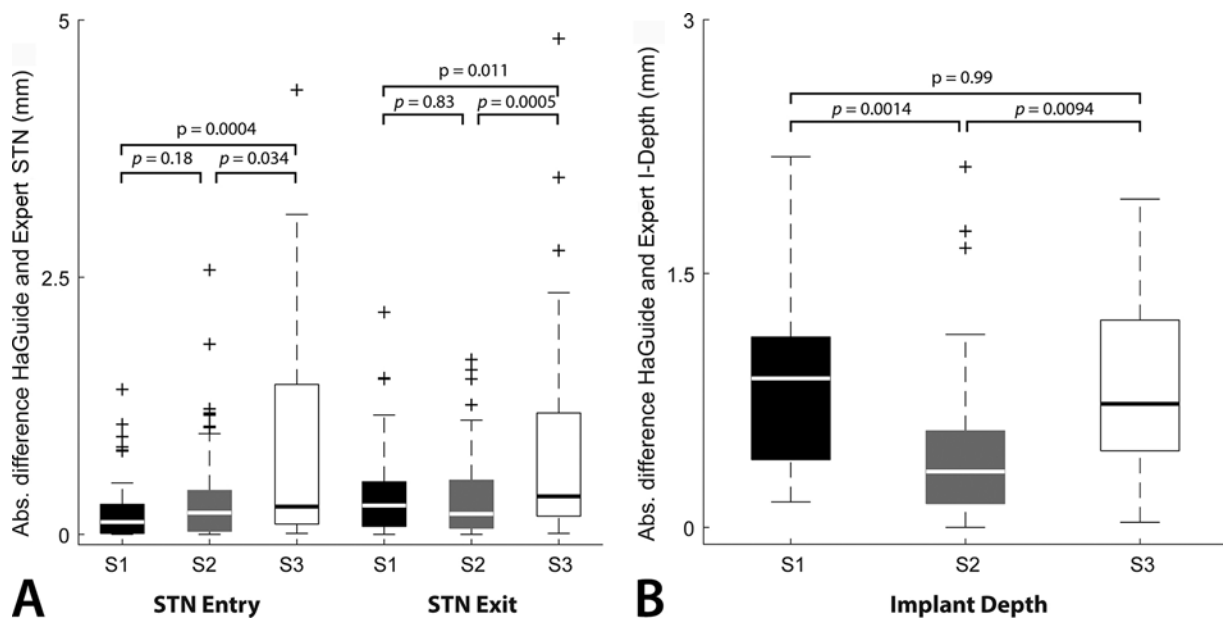


FIG. 5. A: Comparison of absolute differences for the entry into and exit from STN between HaGuide and expert separated by study site. The site estimates for entry into STN showed a group effect ($p = 0.0006$), and post hoc analyses indicated that both site 1 and site 2 differed from site 3 ($p = 0.03$ and $p = 0.0003$, respectively). The site estimates for exit from the STN showed a group effect ($p = 0.0005$), and post hoc analyses indicated that both site 1 and site 2 differed from site 3 ($p = 0.0004$ and $p = 0.01$, respectively). **B:** Comparison of absolute differences for the implant depth of the DBS electrode between HaGuide and expert separated by study site. The site estimates for entry into STN showed a group effect ($p = 0.0003$), and post hoc analyses indicated that both site 1 and site 3 differed from site 2 ($p = 0.001$ and $p = 0.009$, respectively).

Our results from 4 high-volume DBS neurosurgeons highlight the variability associated with selection of implant depth for the STN-DBS electrode (Fig. 4A). Although estimating the implant depth for the DBS electrode varies substantially from expert to expert, when similar implant tracks were selected between expert and HaGuide (83%), the estimates were significantly correlated (Fig. 4B). The default software algorithm strategy relies on detecting the motor domain via increased beta-band activity, to determine the optimal positioning of the ventral-most contact of the DBS lead, taking into consideration the coverage of the entire motor territory of the STN, with as many contacts as possible to provide greater options for DBS programming. Usually, given the average length of trajectories through the STN motor territory, this approach allows for at most 2 contacts (the second and third most ventral/caudal contacts) to be situated within the motor territory, one below the motor territory (i.e., within the STN non-motor domain), and finally, the most dorsal contact at the zona incerta above the STN.⁹

Study Limitations

Conclusions drawn from this study should be tempered by the limitations inherent to a retrospective, post hoc analysis design. In addition, these data were derived from a limited number of study sites; therefore, it remains to be seen whether the results generalize to other DBS centers. Furthermore, statistically significant differences were observed for HaGuide accuracy between sites (Fig. 5A), which could have implications for whether certain surgical strategies or approaches related to STN-DBS differentially

impact HaGuide estimates for STN localization. Simulated study results were collected independent from the intraoperative surgical assessments generated during the surgery. Regarding the implementation of the software, one limitation of the algorithm is that it relies on calculating a reliably differentiable NRMS value as the primary parameter for STN detection. Although more robust than single-unit MER, the measurement of NRMS to detect the STN is sensitive to physiological changes induced by anesthetic agents, such as propofol. Propofol has been shown to affect neuronal activity levels and the background modulation in MER, and therefore the use of propofol may interfere with the results of the software analysis of MER.²⁴ The ability of the software to estimate the optimal track and depth for implantation is limited to trajectories inside of the STN, and it will not account for suboptimal planning or brain shift. Finally, although the software proved to be highly concordant with the selections of the experienced implanting teams, it is currently limited to the STN target in patients with PD. Further studies need to be conducted to improve the algorithm to support the identification of other targets.

Conclusions

In summary, the real-time software algorithm investigated here gives objective and reliable results that can assist new electrophysiologists and surgeons. The software provides information for differentiating the dorsolateral oscillatory region of the STN (motor domain), yielding a complementary adjunct to current techniques of MER, macrostimulation, and motor testing. Efforts are ongoing

to provide similar predictive algorithms to assist with the implantation of DBS electrodes into other commonly targeted brain areas: the ventral-intermediate thalamus for essential tremor and the globus pallidus internal segment for dystonia and PD.

Acknowledgments

This work was supported by grants from the Israel-US Binational Science Foundation, the Adelis Foundation, and the Magnet program of the Office of the Chief Scientist of the Israel Ministry of Economy to Z.I. and H.B.; and the Canadian Friends of the Hebrew University, the Rosetrees and Vorst Foundations, and the Simone and Bernard Guttman Chair in Brain Research to H.B.

References

1. Abosch A, Hutchison WD, Saint-Cyr JA, Dostrovsky JO, Lozano AM: Movement-related neurons of the subthalamic nucleus in patients with Parkinson disease. *J Neurosurg* **97**:1167–1172, 2002
2. Abosch A, Timmermann L, Bartley S, Rietkerk HG, Whiting D, Connolly PJ, et al: An international survey of deep brain stimulation procedural steps. *Stereotact Funct Neurosurg* **91**:1–11, 2013
3. Benabid AL, Benazzouz A, Hoffmann D, Limousin P, Krack P, Pollak P: Long-term electrical inhibition of deep brain targets in movement disorders. *Mov Disord* **13** (Suppl 3):119–125, 1998
4. Benabid AL, Chabardes S, Mitrofanis J, Pollak P: Deep brain stimulation of the subthalamic nucleus for the treatment of Parkinson's disease. *Lancet Neurol* **8**:67–81, 2009
5. Brown P: Oscillatory nature of human basal ganglia activity: relationship to the pathophysiology of Parkinson's disease. *Mov Disord* **18**:357–363, 2003
6. Brown P, Williams D: Basal ganglia local field potential activity: character and functional significance in the human. *Clin Neurophysiol* **116**:2510–2519, 2005
7. Deuschl G, Schade-Brittinger C, Krack P, Volkmann J, Schäfer H, Bötzel K, et al: A randomized trial of deep-brain stimulation for Parkinson's disease. *N Engl J Med* **355**:896–908, 2006
8. Groiss SJ, Wojtecki L, Südmeyer M, Schnitzler A: Deep brain stimulation in Parkinson's disease. *Ther Adv Neurol Disorder* **2**:20–28, 2009
9. Gross RE, Krack P, Rodriguez-Oroz MC, Rezai AR, Benabid AL: Electrophysiological mapping for the implantation of deep brain stimulators for Parkinson's disease and tremor. *Mov Disord* **21** (Suppl 14):S259–S283, 2006
10. Hamel W, Köppen JA, Alesch F, Antonini A, Barcia JA, Bergman H, et al: Targeting of the subthalamic nucleus for deep brain stimulation: a survey among Parkinson disease specialists. *World Neurosurg* **99**:41–46, 2017
11. Hammond C, Bergman H, Brown P: Pathological synchronization in Parkinson's disease: networks, models and treatments. *Trends Neurosci* **30**:357–364, 2007
12. Horn A, Neumann WJ, Degen K, Schneider GH, Kühn AA: Toward an electrophysiological "sweet spot" for deep brain stimulation in the subthalamic nucleus. *Hum Brain Mapp* [epub ahead of print], 2017
13. Hutchison WD, Allan RJ, Opitz H, Levy R, Dostrovsky JO, Lang AE, et al: Neurophysiological identification of the subthalamic nucleus in surgery for Parkinson's disease. *Ann Neurol* **44**:622–628, 1998
14. Krack P, Batir A, Van Blercom N, Chabardes S, Fraix V, Ardouin C, et al: Five-year follow-up of bilateral stimulation of the subthalamic nucleus in advanced Parkinson's disease. *N Engl J Med* **349**:1925–1934, 2003
15. Kulisevsky J, Berthier ML, Gironell A, Pascual-Sedano B, Molet J, Parés P: Mania following deep brain stimulation for Parkinson's disease. *Neurology* **59**:1421–1424, 2002
16. Limousin P, Krack P, Pollak P, Benazzouz A, Ardouin C, Hoffmann D, et al: Electrical stimulation of the subthalamic nucleus in advanced Parkinson's disease. *N Engl J Med* **339**:1105–1111, 1998
17. Little S, Brown P: The functional role of beta oscillations in Parkinson's disease. *Parkinsonism Relat Disord* **20** (Suppl 1):S44–S48, 2014
18. Mallet L, Schüpbach M, N'Diaye K, Remy P, Bardinet E, Czernecki V, et al: Stimulation of subterritories of the subthalamic nucleus reveals its role in the integration of the emotional and motor aspects of behavior. *Proc Natl Acad Sci U S A* **104**:10661–10666, 2007
19. Moran A, Bar-Gad I, Bergman H, Israel Z: Real-time refinement of subthalamic nucleus targeting using Bayesian decision-making on the root mean square measure. *Mov Disord* **21**:1425–1431, 2006
20. Novak P, Daniluk S, Ellias SA, Nazzaro JM: Detection of the subthalamic nucleus in microelectrographic recordings in Parkinson disease using the high-frequency (> 500 Hz) neuronal background. Technical note. *J Neurosurg* **106**:175–179, 2007
21. Odekerken VJ, van Laar T, Staal MJ, Mosch A, Hoffmann CF, Nijssen PC, et al: Subthalamic nucleus versus globus pallidus bilateral deep brain stimulation for advanced Parkinson's disease (NSTAPS study): a randomised controlled trial. *Lancet Neurol* **12**:37–44, 2013
22. Pinzon-Morales RD, Orozco-Gutierrez AA, Castellanos-Dominguez G: Novel signal-dependent filter bank method for identification of multiple basal ganglia nuclei in Parkinsonian patients. *J Neural Eng* **8**:36026, 2011
23. Raucher-Chéné D, Charrel CL, de Maindreville AD, Limosin F: Manic episode with psychotic symptoms in a patient with Parkinson's disease treated by subthalamic nucleus stimulation: improvement on switching the target. *J Neurol Sci* **273**:116–117, 2008
24. Raz A, Eimerl D, Zaidel A, Bergman H, Israel Z: Propofol decreases neuronal population spiking activity in the subthalamic nucleus of Parkinsonian patients. *Anesth Analg* **111**:1285–1289, 2010
25. Rodriguez-Oroz MC, Rodriguez M, Guridi J, Mewes K, Chockkman V, Vitek J, et al: The subthalamic nucleus in Parkinson's disease: somatotopic organization and physiological characteristics. *Brain* **124**:1777–1790, 2001
26. Shamir RR, Zaidel A, Joskowicz L, Bergman H, Israel Z: Microelectrode recording duration and spatial density constraints for automatic targeting of the subthalamic nucleus. *Stereotact Funct Neurosurg* **90**:325–334, 2012
27. Sterio D, Zonenshayn M, Mogilner AY, Rezai AR, Kiprovska K, Kelly PJ, et al: Neurophysiological refinement of subthalamic nucleus targeting. *Neurosurgery* **50**:58–69, 2002
28. Telkes I, Jimenez-Shahed J, Viswanathan A, Abosch A, Ince NF: Prediction of STN-DBS electrode implantation track in Parkinson's disease by using local field potentials. *Front Neurosci* **10**:198, 2016
29. Thompson JA, Lanctin D, Ince NF, Abosch A: Clinical implications of local field potentials for understanding and treating movement disorders. *Stereotact Funct Neurosurg* **92**:251–263, 2014
30. Valsky D, Marmor-Levin O, Deffains M, Eitan R, Blackwell KT, Bergman H, et al: Stop! Border ahead: Automatic detection of subthalamic exit during deep brain stimulation surgery. *Mov Disord* **32**:70–79, 2017
31. Walter BL, Vitek JL: Surgical treatment for Parkinson's disease. *Lancet Neurol* **3**:719–728, 2004
32. Weinberger M, Mahant N, Hutchison WD, Lozano AM, Moro E, Hodaie M, et al: Beta oscillatory activity in the subthalamic nucleus and its relation to dopaminergic

- response in Parkinson's disease. *J Neurophysiol* **96**:3248–3256, 2006
33. Wong S, Baltuch GH, Jaggi JL, Danish SF: Functional localization and visualization of the subthalamic nucleus from microelectrode recordings acquired during DBS surgery with unsupervised machine learning. *J Neural Eng* **6**:026006, 2009
 34. Zaihel A, Spivak A, Grieb B, Bergman H, Israel Z: Subthalamic span of beta oscillations predicts deep brain stimulation efficacy for patients with Parkinson's disease. *Brain* **133**:2007–2021, 2010
 35. Zaihel A, Spivak A, Shpigelman L, Bergman H, Israel Z: Delimiting subterritories of the human subthalamic nucleus by means of microelectrode recordings and a hidden Markov model. *Mov Disord* **24**:1785–1793, 2009
 36. Zhang S, Zhou P, Jiang S, Wang W, Li P: Interleaving subthalamic nucleus deep brain stimulation to avoid side effects while achieving satisfactory motor benefits in Parkinson disease: a report of 12 cases. *Medicine (Baltimore)* **95**:e5575, 2016

Disclosures

Dr. John Thompson reports receiving funding from Alpha Omega for this study. Salam Oukal is an employee of Alpha Omega. Dr.

Hagai Bergman reports receiving funding from Alpha Omega and serving as a consultant for Alpha Omega. Dr. Steven Ojemann reports receiving an honorarium from Alpha Omega for a presentation and serving as a consultant to both Alpha Omega and Medtronic. Dr. Adam Hebb reports a consultant relationship with Alpha Omega. Dr. Sara Hanrahan reports receiving funding from Alpha Omega for this study. Dr. Zvi Israel reports serving as a consultant for Alpha Omega. Dr. Aviva Abosch reports a consultant relationship with Medtronic, receipt of clinical or research support (for study described) from Alpha Omega, and receipt of an honorarium from Alpha Omega for a presentation.

Author Contributions

Conception and design: Thompson, Bergman. Acquisition of data: all authors. Analysis and interpretation of data: Thompson, Oukal, Bergman. Drafting the article: Thompson, Oukal. Critically revising the article: Thompson, Oukal, Bergman, Israel, Abosch. Reviewed submitted version of manuscript: all authors. Approved the final version of the manuscript on behalf of all authors: Thompson. Statistical analysis: Thompson. Study supervision: Abosch.

Correspondence

John A. Thompson: University of Colorado School of Medicine, Aurora, CO. john.a.thompson@ucdenver.edu.